Atteia olivier (Orcid ID: 0000-0002-2096-6908)
Vlassopoulos Dimitri (Orcid ID: 0000-0002-6448-7685)

Research Paper

muFlowReacT: A Library to Solve Multiphase Multicomponent Reactive Transport on Unstructured Meshes 5.1

O. Atteia
Corresponding author: UMR EPOC, Bordeaux-INP, 1 Allee Daguin, 33607 Pessac Cedex, France; Email: olivier.atteia@ensegid.fr

H. Prommer

School of Earth Sciences, University of Western Australia, Crawley, Western Australia, Australia; CSIRO Land and Water, Floreat, Western Australia, Australia.

D. Vlassopoulos

Anchor QEA, LLC, Portland, Oregon USA

L. André

BRGM, Water Service, Orléans, France.

G. Cohen
UMR EPOC, Bordeaux-INP, 1 Allee Daguin, 33607 Pessac Cedex, France

Conflict of interest: no conflict of interest identified

Key words: OpenFoam, Phreeqc, groundwater, dual phase, diffusion

Article Impact Statement: *This paper shows the setup of a new reactive code coupling OpenFoam and Phreeqc with specific abilities to solve small dispersion in unstructured mesh, and reactive gas transport.*

Abstract

In this paper we present a new reactive transport code for the efficient simulation of groundwater quality problems. The new code couples the two previously existing tools OpenFoam and PhreeqcRM. 5.3 The major objective of the development was to transfer and expand the capabilities of the MODFLOW/MT3DMS-family of codes, especially their outstanding ability to suppress numerical dispersion, to a versatile and computationally efficient code for unstructured grids. Owing to the numerous, previously existing transport solvers

This article has been accepted for publication and undergone full peer review but has not been through the copyediting, typesetting, pagination and proofreading process which may lead to differences between this version and the Version of Record. Please cite this article as doi: 10.1111/gwat.13345

contained in OpenFoam, the newly developed code achieves this objective and provides a solid basis for future expansions of the code capabilities. The flexibility of the OpenFoam framework is illustrated by the addition of diffusional processes for gaseous compounds in the unsaturated zone and the advection of gases (multi-phase transport). The code capabilities and accuracy are illustrated through several examples: (i) a simple 2D case for conservative solute transport under saturated conditions, (ii) a gas diffusion case with reactions in the unsaturated zone, (iii) a hydrogeologically complex 3D reactive transport problem and finally (iv) the injection of CO_2 into a deep aquifer with acidification being buffered by carbonate minerals.

Introduction

Reactive transport modeling has shown to be an increasingly important tool in research and for groundwater practitioners to integrate, interpret and predict coupled groundwater flow, solute transport and (bio)geochemical reaction processes (e.g., Prommer et al. 2019; Sun et al. 2020; Siade et al. 2021; Schafer et al. 2021). However, model applications to real three-dimensional systems with spatial complexity have remained a formidable endeavor. To date, one of the key challenges in heterogeneous systems is, even in the absence of reactive processes, to solve the transport equation itself, in many cases the classic advection-dispersion equation (ADE). Over the last three decades MT3D (Zheng 1990) and later MT3DMS (Zheng and Wang 1999) have, for many good reasons, been the most widely used solvers for solute transport problems in groundwater systems. This is not only a result of their seamless compatibility with all earlier MODFLOW versions (Harbaugh 2005), but also of their outstanding robustness (Zheng et al. 2012) and, importantly, the availability of multiple solvers for the advection term, with each of them having their individual strengths and weaknesses under varying conditions, often strongly depending on the degree of spatial discretization of the problem.

Until recently, the dominance of MODFLOW-based codes in solving real-world groundwater flow and quality problems, has somewhat suppressed the needs and opportunities to exploit the advantages of highly efficient generic multi-physics codes that were developed outside the groundwater community for applications to a wide range of related science/engineering disciplines. One of these codes is OpenFoam (Weller et al. 1998), a free (available under the GNU license) and open source software with an open structure that supports the solution of multi-physics computational fluid dynamics (CFD) problems. Importantly, spatial discretization of any simulation problem is handled in OpenFoam via structured or unstructured meshes. Compared to the traditional MODFLOW-based solute and reactive transport codes, such as MT3DMS, SEAWAT, RT3D and PHT3D, there are several advantages of OpenFoam:

(i) a finite volume solution approach allowing for complex geometries (present in recent versions of MODFLOW but not in associated reactive transport codes)

(ii) a modular approach that allows for rapid inclusion of new equations or processes that address complex behavior,

(iii) multiple transport solvers that provide for faster and more accurate solutions in the finite volume domain

(iv) built-in parallelization to solve the defined equations (also present now in some MODFLOW Solvers, see, e.g., Dong and Li 2009, Sun et al. 2019) and,

(v) handling of equations written in a format very close to their mathematical formulation, thereby allowing addition of new functionality, as often required by advanced users.

Recently, two OpenFoam libraries were developed for geochemical reactions, for equilibrium reactions (Maes and Menke 2021), or through coupling with PHREEQC (Pavuluri et al. 2022). These libraries are intended to solve pore scale problems, therefore they lack many groundwater- or surface water specific simulation capabilities (e.g., general head boundary

conditions, rivers and drains) that resemble that of the MODFLOW/MT3DMS family of codes. Perhaps most significantly, the library does not allow to simulate unconfined groundwater flow systems, which is a severe limitation. In order to equip OpenFoam with suitable geochemical reaction capabilities, we followed the path of earlier coupling efforts in applying a sequential operator splitting approach (e.g., Walter et al. 1994, Jacques et al. 2012) and employed the USGS code PHREEQC as reaction simulator (e.g., Appelo and Willemsen 1987; Prommer et al. 2003; Parkhurst et al. 2010; Lu et al. 2022; Healy et al. 2018; Muniruzzaman and Rolle 2019; De Sousa 2012). Indeed, the popularity of coupling PHREEQC to flow/solute transport simulators has triggered the USGS to develop and release the PhreeqcRM API (available under GNU license), aimed at simplifying the mechanics of model coupling (Parkhurst and Wissmeier 2015). The reasons for the popularity of using PHREEQC as reaction module for the computation of geochemical processes are manifold:

(i) it is distributed with a variety of thoroughly reviewed and validated thermodynamic databases,

(ii) it has a built-in BASIC interpreter, allowing for a highly flexible definition of complex reaction rate laws and output post-processing options, and

(iii) the ability to handle calculations involving solution density, rock volume, and partially saturated porous medium.

Clearly, there remains a strong need for an efficient PHREEQC-based reactive transport simulator that can simultaneously overcome the apparent disadvantages of structured grids while achieving an accurate solution of the solute transport problem under challenging conditions. This paper reports the development and main features of muFlowReacT (muRT, freely available under the GNU license), a code which (i) significantly expands the capabilities of OpenFoam towards a versatile groundwater flow and solute transport simulator and (ii)

couples PhreeqcRM to OpenFoam to allow for the simultaneous simulation of a wide range of (bio)geochemical processes that can affect groundwater quality.

In this paper, we first present the formulation of the equations used in the OpenFoam framework, and the methods for treating boundary conditions, followed by the presentation of the employed coupling strategy between OpenFoam and PhreeqcRM. The third section is devoted to the presentation of four selected modelling problems that demonstrate the code's simulation capabilities and the attained numerical accuracy:

(i) a 2D example where a direct comparison with an exact analytical solution is possible,

(ii) a 1D problem that illustrates reactive transport under variable saturated conditions and in the presence of dispersive gas transfer,

(iii) a larger-scale 3D reactive transport problem under complex hydrogeological conditions, and finally

(iv) a radial flow and reactive transport example involving gas injection (CO_2 at high pressure) and mineral dissolution.

Research method

Mathematical formulation

Here we provide a brief overview of the governing flow and transport equations that are solved. While these equations are all well known, they are presented here in the light of some specific formulations that were adopted to use OpenFoam as a general framework that can seamlessly exchange information with PhreeqcRM.

Single phase flow

The governing equations for flow and transport are solved by OpenFoam. For single phase flow, the model solves the diffusivity equation expressed in head:

$$\boldsymbol{S_h \cdot \frac{\partial h}{\partial t} - \nabla\left(M_f \nabla h\right) + \nabla \Phi_{Gr} = Q} \quad (1)$$

where S_h is the storage term, M_f the mobility, Φ_{Gr} the vector of gravity flow linked here to potential density variation and Q the flow source term. Here, $M_f = \frac{k\rho|g|}{\mu}$ where k is the permeability tensor (m^2), ρ the density ($kg.m^{-3}$) and μ the dynamic fluid viscosity ($kg.m^{-1}.s^{-1}$). In the classical formulation of the flow equation in a finite volume, the anisotropic parameters are expressed as tensors. In OpenFoam, the tensor operation to set the equation for a given geometry is transparent: OpenFoam calculates the product of the tensor parameters with the surface vector of each cell face to determine M_f at the cell faces. This differs fundamentally from the approach employed by the MODFLOW family of codes, including MODFLOW-USG: In OpenFoam it is assumed that the hydraulic conductivity anisotropy is not oriented according to the horizontal direction but is parallel to the model layer, even if the layer is tilted. A specific option for the permeability field was therefore adopted in muRT to reproduce this behavior. For the inter-layer faces the hydraulic conductivity is set to the value of K_v (vertical hydraulic conductivity) regardless of whether the face is horizontal or tilted. At the same time, harmonic averaging is performed.

$$\Phi_{Gr} = \frac{k\rho}{\mu} \cdot g \quad (2)$$

where g is the gravity vector. If required, equation (1) can be solved without the temporal term in order to simulate steady state flow. In OpenFoam, the SIMPLE solver (Mangani et al. 2014) is used, which includes both linear and non-linear equations to solve for steady state conditions.

For unconfined flow, the relative saturated thickness is calculated as (McDonald and Harbaugh 1988):

$$\boldsymbol{h_w = \frac{h - z_{bot}}{thk}} \quad (3)$$

where h is the hydraulic head in the considered cell (m), z_{bot} is the bottom elevation of the cell (m), *thk* its thickness (m) and $h_w$is the relative saturated thickness (-). The value of $h_w$is bounded between 10^{-4} (dry cells) and 1 (fully saturated). In equation (1), h_w decreases the section for flow and thus $M_f = h_w \frac{k\rho|g|}{\mu}$ in case of unconfined flow. In contrast, $h_w$is simply set to 1 over the rest of the domain. It is evident that this part of the equation cannot be solved implicitly, and thus $h_w$is recalculated at each time step. As in MODFLOW, the employed storage coefficient differs, depending on whether a cell is confined or unconfined.

Unsaturated flow

For an unsaturated porous medium, the major variable is h_p, the pressure head, and, by analogy to Eq. 1, the equation is (Bear 1988):

$$C_h \cdot \frac{\partial h_p}{\partial t} - \nabla\left(M_f \nabla h_p\right) + \nabla \Phi_G = Q \quad (4)$$

Here the storage coefficient is replaced by C_h, the capillary capacity, with (Nielsen et al. 1986):

$$C_h = \alpha \cdot m \frac{sw_x - sw_n}{1-m} {S_e}^{1/m}\left(1 - {S_e}^{1/m}\right)^m \quad (5)$$

sw is the water saturation, sw_x its maximum value and sw_n its minimum and *Se* is the effective saturation expressed as

$$S_e = \frac{sw - sw_n}{sw_x - sw_n} \quad (6)$$

where α and *m* are the van Genuchten coefficients of the capillary curve (van Genuchten, 1980).

Two-phase flow

In its present formulation, the muRT library includes a general capability to simulate multiphase flow, albeit its current implementation is limited to two phases (water and gas). The mathematical formulation was directly adopted from Horgue et al. (2015):

$$-\nabla\left(M_f \nabla P_g\right) + \nabla\Phi_{Gr} - \nabla\Phi_{pc} = Q_g \quad (7)$$

and

$$\varepsilon \frac{\partial sw}{\partial t} + \nabla\Phi_w = Q_w \quad (8)$$

where P_g is the gas pressure, ε the porosity, and Φ_{pc} and Φ_w are the capillary and water fluxes, respectively, across the cell face. Here, the fluid mobility M_f is the total mobility which includes water and gas. The two equations are solved iteratively with the pressure term being implicit and the flux term being explicit in eq. 7. For eq. 8, the *sw* term is implicit and the other terms are explicit. This is a classic approach in the multiphase literature and was previously shown to be as efficient as the fully implicit approach at a lower computational effort for most cases (Chen et al., 2006)."The classical formulation of relative permeability is used (Mualem 1986).

Solute transport

As in most reactive transport frameworks (e.g., PHT3D, MIN3P), solute transport simulations are performed for total aqueous component concentrations C_i (Yeh and Tripathi 1991; Engesgaard and Kipp 1992), defined as:

$$C_i = c_i + \sum_{j=1}^{ns} Y_j^s \, s_j \quad (9)$$

where c_i is the molar concentration of the (uncomplexed) aqueous component, n_s is the number of species in dissolved form that have complexed with the aqueous component, Y_j^s is the

stoichiometric coefficient of the aqueous component in the j^{th} complexed species and s_j is the molar concentration of the j^{th} complexed species.

The transport of the total component concentrations is based on (Zheng and Bennett 2002):

$$\theta_j \frac{\partial C_{i,j}}{\partial t} + C_{i,j} \frac{\partial \theta_j}{\partial t} + \nabla\left(\Phi_j C_{i,j}\right) - \nabla\left(\theta_j D_j \nabla C_{i,j}\right) = Q \quad (10)$$

where $C_{i,j}$ is the concentration of component i in fluid phase j (aqueous or gas), θ_j is the fluid content $(\varepsilon.sw)$, Φ_j is the fluid phase flux and D_j the dispersion tensor. D_j includes both dispersion and diffusion (Bear 1988). In the gas phase, the effective diffusion is calculated using the Millington and Quirk formulation (Millington 1959). Q is the source term, which may include mass exchange with rivers, drains, across constant head boundaries or wells, but, importantly for muRT, also chemical reactions. Here, all terms are implicit, except for Φ_i, which is explicit, coming from the solution to the flow equation.

For a system of n chemical components, eq. 10 for i varying from 1 to n are solved separately, as the concentration gradient differs for each component.

Numerical Implementation

Overview

OpenFoam is written in C++ with a modular structure, which allows the user to program its own set of equations and use the finite volume tools embedded in OpenFoam to solve the specified problem. Although the basis of the transport equation was inspired by the previous work of Horgue et al. (2015), the structure of the muRT library is completely different, having been developed specifically for the conditions encountered for flow in aquifers and multi-component reactive transport.

Geometry

Although OpenFoam can, in principle, use polyhedra of any shape, in the present implementation of muRT the definition of the cell geometry is limited in two ways:

- Each cell within any layer has a corresponding cell of the same projected geometry (i.e., the faces between cells in the same layer are all vertical). However, in contrast to the formulation employed in MODFLOW, the tops and bottoms of cells strictly correspond to the layer topography.
- Each face can only link two adjacent cells, i.e., it is not possible to have one cell on one side and two cells on the other side, as in nested grids.

The current implementation of muRT uses the Voronoi mesh, primarily because it allows for a more accurate solution of the solute transport problem (Vrettos et al. 1989). For calculations involving a value at a cell's face, OpenFoam allows choosing among several interpolation options to obtain the value at the face.

Boundary and internal conditions

OpenFoam, like MIN3P (Mayer 2002), adopts a definition of boundary conditions in which (i) these can only be defined at domain boundary cells and (ii) they apply at the outside of cell boundaries, not in the center of the cells. In the groundwater literature there has historically been a misuse of the term "boundary condition", which often is employed for not only the domain boundary itself but also within the domain. This may lead to some differences in simulation results, especially for coarse spatial discretization. Importantly, this contrasts the formulation employed in the MODFLOW family of codes, which also allow for the formulation of boundary conditions inside of a model domain.

In order to set specific properties inside a domain, OpenFoam uses the fvOptions paradigm. This concept allows to append information directly into the solver matrix. We developed

specific fvOptions constraints to specify heads, or pressures, and concentrations as "boundary conditions", similar to their definition in the MODFLOW/MT3DMS family of codes. The second type of option "source" was used to specify a source term, whether directly (Neuman condition) for wells or surface recharge, or in relation to the value of the considered variable (head or concentration) in the corresponding cell (Cauchy condition) for source/sinks such as rivers or drains.

Coupling of OpenFoam and PhreeqcRM

In muRT, the coupling between OpenFoam and PhreeqcRM is achieved through a sequential operator-split technique (Yeh and Tripathi 1991, Barry et al. 2002), a routinely used strategy to equip solute transport simulators with geochemical reaction capabilities. Since 2015, the US Geological Survey provides an API (PhreeqcRM) of the stand-alone PHREEQC version (Parkhurst and Appelo 2013). The API substantially simplifies the integration of its components into other codes (Parkhurst and Wissmeier 2015) and several coupled codes that employ PhreeqcRM have been developed and presented since then (e.g., Healy et al. 2018; Muniruzzaman and Rolle 2019). In muRT, the Phreeqc API has been included as an OpenFoam class that can be called whenever required. For reactive transport problems that involve mobile and immobile entities, concentrations of immobile entities associated with the solid phase, such as mineral phases, exchange sites, and surfaces, are stored in the PhreeqcRM class, while the concentrations of any mobile entity is sequentially exchanged between OpenFoam and PhreeqcRM, similar to other reactive transport codes (e.g., Prommer et al. 2003; Xu et al. 2012).

PhreeqcRM uses total aqueous component concentrations C_i, as defined by Eq. 8, as inputs for reaction calculations. In order to maintain electron balance, density effects, ionic strength effects, and to compute the pH or pe, PhreeqcRM stores and uses the concentrations of water, oxygen and hydrogen and of any charge imbalance. The muRT library is based on the aqueous

components and thus requires an initial execution of PhreeqcRM in order to calculate the concentrations of all components from the Phreeqc solution definitions within the domain.

For two-phase systems with pressure variations in the gas phase, special care must be taken as reactions can modify the amount of the gas components. Each PhreeqcRM cell receives the porosity, the current water saturation, volume of the gas phase and partial pressure of each gas species from OpenFoam, as computed during the previous time step. Each PhreeqcRM reaction calculation is performed in constant volume mode, which can produce variations in partial pressures that results from progressing reactions. Thus, the final resulting pressure (the sum of all partial pressures) is transferred back to OpenFoam. In the next calculation step, the pressure equation is solved to equilibrate the pressure with the surrounding cells and then the saturation equation is solved where water from neighboring cells moves to equilibrate pressure.

Several options have been implemented to reduce the computational load. First, it is possible to solve the reactive transport equations in a specified subdomain of the groundwater flow domain. Second, changes in concentrations in each cell within the reactive transport subdomain between subsequent time steps are tracked and PhreeqcRM is called only when the concentration of at least one aqueous component has changed by more than a user-specified threshold value.

Schemes, solutions and solvers

OpenFoam implements several advection schemes, such as the van Leer scheme (Van Leer 1974) and other higher order solvers derived from the total variance diminishing (TVD) approach, like SuperBee or MUSCL (Darwish and Moukalled 2003) to deal with the earlier mentioned and often encountered difficulties in numerically solving the advection-dispersion equation. In muRT, we slightly modified the SuperBee algorithm by setting at each step the few slightly negative concentrations to zero ones but this artificial negative mass is removed from other cells in order to keep the total mass.

OpenFoam also provides several linear solvers that can be specified for each of the used equations. Here, PCG was mainly used for head or pressure and BiCGStab for concentrations. The pre-conditioners can also be chosen according to the solver and problem. In the same input file, the absolute and relative tolerances and the maximum number of time steps can also be specified. For non-linear problems like unsaturated and dual phase, we used the Picard approach brought by Horgue et al. (2015).

In the present implementation of the unconfined flow solution equation, piecewise curves were added in the relative wet thickness *hw* in order to smooth the function at the point of sharp change of *hw* slope according to head (similar to the one described in Panday 2017). This helps to stabilize the outer iterations.

The time stepping for the unsaturated and dual phase flow solutions are adaptative, based on the computed Courant numbers (Horgue et al., 2015). In OpenFoam, the transport time stepping is adapted by using a tolerance on the relative concentration variation over two consecutive time steps (default value is 1×10^{-3}). Given that a SNIA (Sequential Non-Iterative Approach) is employed to couple transport and chemistry, it was not viable to incorporate an automatic and time step definition. However, to adjust the computational load while monitoring accuracy, it is possible to select the frequency at which reaction steps are performed relative to the transport time steps.

Overall structure

The structure of the muRT library is illustrated in Figure 1. In muRT, in order to allow flexibility, the options for each process are independent, i.e., it is possible to select a different type of flow solver for each transport solver. Thermal effects can also be modeled for any flow or transport option. Chemistry is only associated with multi-component transport for dissolved or gaseous components.

Illustrative Application Examples

Selected model application examples are presented below in order to illustrate the comprehensive range of simulation capabilities that are included in muRT. All individual model simulation results are benchmarked against numerical codes that can correspondingly handle the specific processes that are included in each of the application examples. The specifically tested and presented capabilities illustrate the achieved accuracy in solving conservative solute transport problems as well as reactive transport in the unsaturated zone and in multi-phase systems. This highlights that muRT combines the capabilities of several specialized codes while achieving accurate results effectively.

Case 1: 2D conservative transport in a uniform flow-field

This first illustrative example demonstrates muRT's abilities in solving the transport of conservative solutes. The example involves the instantaneous pulse-type injection of a tracer into an aquifer discretized by a regular mesh that is characterized by a uniform flow field. The simulated groundwater flow occurs in diagonal direction. This setup was selected to specifically demonstrate muRT's performance for the typical "real world" case, where groundwater flow does not occur parallel to the mesh discretization direction. With the longitudinal and transverse dispersivities set to 0.5 and 0.05 m, respectively, the transport is advection dominated. The solution obtained by muRT is compared with the solution obtained by MT3DMS, whereby comparable spatial discretization levels were employed. In MT3DMS, which was discretized by a regular grid, cell sizes were set to 1 × 1 m, thus being larger than the dispersivity values, similar to what is typical for many real world cases (e.g., Seibert et al. 2016; Sliwka et al. 2005). Two of MT3DMS's advection schemes were tested, i.e., TVD and MOC, while the finite difference advection scheme was excluded as it well known to poorly perform for advection-dominated problems. In muRT and MODFLOW-USG Voronoi polygons were used for spatial discretization, with a Delaunay triangulation provided by Gmesh (Gueuzaine et al. 2009) (see

Supporting Information (SI) for the mesh geometry). The employed number of cells (11831) was similar to that of the MT3DMS model (10000), i.e., the size of each cell is close to 1 m^2. A comparison with Feflow (Diersch 2014) was also added, as it is a widely used flow and solute transport model.

Figure 2 shows a comparison of simulation results obtained with MT3DMS (TVD and MOC), with those obtained using a Voronoi mesh (muRT and MODFLOW-USG) and an analytical solution of the problem. Solute concentrations are presented as profiles along the flow direction and transverse to it. All parameters that were defined for the different solvers are provided in the Supporting Information. Interestingly, due to the low value of the transverse dispersivity (0.05 m), none of the tested numerical models was able to provide a perfect match to the analytical solution. It can be seen that the TVD method, as incorporated in MT3DMS, performs most favorably, while MT3DMS's MOC implementation seems to suffer from a poor mass balance (calculated over the whole domain). OpenFoam's implementation of the van Leer scheme, like Feflow, compares quite well with the TVD results in both cases, i.e., for groundwater flow parallel and diagonal to the principle discretization direction. The SuperBee scheme, which was developed for advection-dominated problems and modified in muRT to avoid negative concentrations, performs very well, mostly matching the analytical solution. Notably, thanks to the correction described above, muRT does not show negative concentrations, in contrast to the TVD or Feflow solutions. MODFLOW-USG shows a much higher numerical dispersion, particularly in the transverse direction, comparable to the classical finite difference upwind scheme. If not constrained, the MODFLOW-USG solver is using an implicit scheme for transport, but tolerance and time step limiting are also available. A wide range of settings were tested, including small time steps (e.g., 10^{-3} d in the 1st step and a maximum of 0.1 d), and for every setting the numerical dispersion remained noticeable. This mainly shows that the group of TVD methods such as MUSCL or SuperBee, that are available

within OpenFoam is capable of dealing with sharp fronts on unstructured meshes, which is unfortunately not very common. The success of MT3DMS can be closely tied to the availability of several alternative options for advection schemes, each suiting best specific combinations of problem type, available memory, etc. Here, OpenFoam shows the same capabilities for unstructured meshes.

For this simple 2D case, model execution times were quite similar among all tested codes. Full model details are provided in the Supporting Information.

Case 2: benzene diffusion in unsaturated soil

This example simulates the pollution spreading that occurs in the presence of a NAPL (Non-Aqueous Phase Liquid) source of a volatile contaminant, pure benzene, above the groundwater table in the vadose zone. During an initial phase of the simulation period, the water content was considered to be at steady state and being at equilibrium with the groundwater table at z=0.01m, before a rainfall event with an infiltration rate of 3×10^{-7} m.s^{-1} was assumed to occur between days 3.2 and 3.8. The source of NAPL benzene was assumed to be at equilibrium with the water and gas phases and therefore benzene slowly diffuses away from the source zone in the water phase and more rapidly in the gas phase. During diffusion, gaseous benzene is also exchanged instantaneously with the water phase according to the equilibrium described by Henry's law (K_h). At the same time, oxygen diffuses downward from the surface and, as a result, biodegradation of benzene can occur at locations where both reagents, i.e., benzene and oxygen, prevail. The reaction, which is assumed to occur in the aqueous phase, is described in this example by commonly used dual Monod kinetics (e.g., Barry et al. 2002):

$$k = k_0 \frac{|O_2|}{(K_{O2}+|O_2|)} \frac{|Bz|}{(K_{bz}+|Bz|)} \quad (11)$$

where k_0 is the reaction constant (d^{-1}), $|O_2|$ and $|Bz|$ are the oxygen and benzene concentrations in water (mol.L^{-1}) respectively, and K_{O2} and K_{bz} are half saturation constants (mol.L^{-1})

For simplicity, neither sorption of benzene onto the solid phase nor NAPL mobility was assumed. The tortuosity in the gas phase is computed based on the Millington empirical relationship, and the diffusion coefficients of the gaseous species were assumed to be the same. The simulation results obtained with muRT are compared with the corresponding results obtained with MIN3P (Mayer 2002).

Figure 3 shows the simulated concentration depth profiles after a simulation time of 3 and 5 days, respectively. For most components the comparison of the results shows only minor differences between the two numerical solutions. At day 3 both models show the same value of benzene partial pressure at z=0.24 m, due to the presence of the NAPL and Henry's law equilibrating water with the gas phase. The presence of benzene in the gas phase leads to vertical diffusion in both directions. However, the diffusion is very limited in the downward direction due to the presence of the water table at the profile bottom. At the top of the simulated depth profile, the gas composition is equilibrated with the atmosphere, i.e., with zero benzene concentration. The diffusion of gaseous benzene from the NAPL source location provides benzene to the aqueous phase, which then reacts with oxygen and produces CO_2. The code comparison (Figure 3) shows only slight differences between the two compared codes.

The effect of the rainfall event is clearly evident in the simulated concentration depth profiles, with similar results for both models. As can be seen, the concentration gradients of the gaseous species are higher in the region of increased water content, which is a result of the reduced gas diffusion coefficient that occurs wtih higher water saturation. However, at elevations between 1.5 and 1.8 m, MIN3P shows much higher partial pressure of oxygen compared to atmospheric pressure. This arises from the fact that in MIN3P there is no gas advection and the infiltration of water increases the gas pressures. In real world infiltration may lead to increasing gas pressures, but they are rapidly equilibrated when water content does not reach the porosity value. In order to mimic this phenomenon in muRT the sum of the gas components partial

pressure is kept constant for unsaturated soil. Note, that when a substantial infiltration event occurs, the infiltrating water can block the gas to below the infiltration front. In such cases the multiphase capability of muRT should be invoked.

As MIN3P employs a global implicit method to solve the flow and reactive transport system, the local equilibrium at the NAPL point between dissolution, volatilization and gas diffusion is solved simultaneously. In contrast, as muRT uses a sequential operator-split approach and the diffusion in the gas phase is relatively rapid, this requires a fine temporal discretization (around 0.01 d) to obtain an accurate solution, i.e., a large number of phreeqcRM executions, which makes muRT much slower than MIN3P for this case.

Case 3: 3D reactive transport with ion exchange

This 3D reactive transport test case assesses the muRT performance under complex hydrogeological conditions that are typical for many real world modelling problems. In the test case, the complexity arises particularly from (i) the widely varying thickness of some model layers, from less than a meter to more than 100's m (ii) the hydraulic conductivity (K) varying in space over several orders of magnitude and (iii) the horizontal to vertical K ratio varying in space. The domain, which represents an unconfined aquifer, includes several internal boundary conditions, which are treated in MODFLOW-USG by a General Head condition (GHB) or drains. Several wells, and particularly one deep well with a very high pumping rate, are used to contain a contaminant plume. The resulting flow pattern that evolves between this well and the adjacent river, which provides significant recharge, are quite complex. In addition, there is also a wide variation of recharge fluxes that are induced by a number of infiltration ponds. Full details of the site characteristics are provided in the Supporting Information.

Figure 4 shows the distribution of hydraulic heads in layers 1 to 5 of the model. The contours are shown for heads of 9, 18, 27, 40 and 50 m (from blue to brown). In layer 2 the position of

the fixed head boundaries, close to 10.3 m are shown in grey, and the large drain region (elevation 13.5 m) is shown by the dash-dotted grey polygon, while the southern boundary was defined as a general head boundary (GHB), set to an elevation of 42 m. Full details are provided in the Supporting Information. Simulated heads are very similar for MODFLOW-USG and muRT for layers 2 to 5, except for selected locations close to the drain, where some small differences occur. In layer 1, a part of the domain is dry, therefore head contours are absent for MODFLOW-USG results, while for muRT calculated heads are shown. It can be seen in the results computed for layer 1, that MODFLOW-USG provides very low values (9 m) south of the drain area, which is specified at 13.5 m. It seems therefore that the muRT solution is more robust than the one provided by MODFLOW-USG. A wide range of solver settings was explored, including a decrease of the tolerance, without clear improvement of the MODFLOW-USG solution.

The conservative transport problem is defined by a dissolved contaminant that is present in the grey zone of layer 2 (see figure) as a continuous source for a period of 50 years. Figure 5 compares the results of both, muRT and MODFLOW-USG. It can be seen that the contaminant plume is effectively captured by the deep well. Although the results are quite similar, it can be seen that the MODFLOW-USG simulated plume disperses slightly more than that simulated by muRT. The small difference, compared to the earlier discussed 2D diagonal case, may be due to the fact that here solute transport occurs in combination with a convergent flow pattern, in which case dispersion remains smaller compared to the case of uniform flow.

Using the same groundwater flow pattern and solute transport parameters, a source composed of the mineral fluorite is defined for the same area for the tracer in the previously described case. For this simulation scenario, it was assumed that an anion exchanger, namely aluminum hydroxide, is uniformly distributed across the entire model domain. The exchanger, referred to as Y, can fix both F (log_k = 0.5 for YF) and P (log_k = 0.4 for Y_3PO_4). This leads to the

sorption and retardation of dissolved fluoride. Downstream of the fluorite source, the spatial distribution of dissolved phosphate, which is present at background levels throughout the domain (detailed chemistry is provided in the Supporting Information) is influenced by the competition for sorption sites on the Y exchanger.

Figure 6 shows the simulation results obtained by muRT and MODFLOW-USG for both, fluoride and phosphorus for layers 2 to 4 (top to bottom). Simulated concentration contours for fluoride are very similar, except for MODFLOW-USG producing a slightly larger plume for the deepest layer (layer 5). For phosphorus, the simulated concentrations also compare well, except for, again, a larger plume extent simulated by MODFLOW-USG at greater depth. These discrepancies indicate that MODFLOW-USG results are slightly more affected by numerical dispersion than muRT.

Case 4: CO_2 injection in a deep well

The last case illustrates the multi-phase modeling capability of muRT. The example is based on earlier work described by André et al. (2007), where the full details for this case can be found. Briefly, pure CO_2 is injected at a pressure of 200 bar and a temperature of 75 °C at a rate of 1 $kg.s^{-1}$ into a deep aquifer. In the model simulations, the aquifer is represented by a radial-symmetric domain. The corresponding volume of gas is calculated by muRT and TOUGHREACT using the Peng Robinson formulation (Robinson et al. 1985), which includes the case of a supercritical state of CO_2. In Figure 7 the water saturation, pH and ion concentrations are shown as a function of distance from the injection well after 10 years of continuous injection.

As can be seen, the gas injection lowers the water saturation in the medium (Figure 7a; left axis), with a diffused front, which is linked both to the employed values of the van Genuchten parameters and also to the radial configuration. Indeed, as the cells sizes increase with distance

from the well, the same gas flux can occur across a cell at lower gas saturation. During the gas injection, a small water flux occurs towards and across the model external boundary: it corresponds to the variation of *Sw,* as the main moving fluid is gas. Therefore, less than a pore volume of water has swept across any cell. The very low values of *Sw* close to the well are due to the injection of a dry gas that leads to a drying of the medium through water evaporation. The saturation patterns are different in the two models and we did not find a clear explanation for this, despite numerous tests in muRT. Both models provide a correct water/gas volume balance.

To simulate the geochemical reactions, the TOUGHREACT chemical database, as provided by André et al. (2007), has been translated to a Phreeqc reaction database. The reactions are first linked to the equilibrium-based dissolution of CO_2 into water, as calculated based on the Peng Robinson formulation for the Henry coefficient. As the pressure and temperature remain close to 200 bar and 75 °C in the entire domain, the Henry coefficient varies barely in space. The high pressure of CO_2 in the injected gas phase leads to an acidification of the water. This acidification is compensated by the buffering effect that is provided by an assemblage of carbonates. Their dissolution and/or precipitation is assumed to be kinetically controlled, using rate laws that were originally proposed by Lasaga and Kirkpatrick (1981), and described in more detail in Andre et al. (2007) as well as in the Supporting Information. The majority of the pH buffering effect results from the presence of calcite and dolomite in the sediment. As each kinetic rate depends on the mineral saturation state, once the equilibration with CO_2 is reached, mineral concentrations do not change any further.

Figure 7a shows that the pH steeply drops at the front where CO_2 is present. Interestingly, the high CO_2 pressure leads to a low pH, even where complete equilibrium with carbonate minerals is attained. The simulated pH profiles agree very closely between the two compared models, muRT and TOUGHREACT. The pH value where CO_2 is present, around 4.8, is controlled by

the induced buffering reactions. Indeed, Phreeqc simulations of CO_2 equilibration without minerals (not shown) lead to a much lower pH. It is interesting to notice that despite the obtained discrepancies in water saturation between muRT and TOUGHREACT, the pH is similar and the front is located at the same place. Very close to the well, the model results differ slightly, due to the very low saturation, which induces complex chemical interactions. However, as barely any water flow occurs at this location the discrepancies have no further implications for the geochemical patterns at larger distances.

Finally, Figures 7b and c show the concentration profiles for dissolved species. Almost all dissolved species behave similar to pH, with a sharp change at the front and mostly stable values closer to the well. The reason for the latter is that at greater radial distances the kinetic rates are faster than the gas displacement due to the elevated temperatures. Moreover, as already discussed above, there is only very limited water movement which induces only minor changes in mineral concentrations and porosity. Contrary to pH, there are some discrepancies between the concentrations of some species, which are quite low for most species but higher for Si. The simulated mineral concentrations pattern is mostly characterized by successively progressing dissolution fronts. However we were not able to obtain a correct mass balance for minerals in TOUGHREACT.

Conclusions

This article presents the development and capabilities of a new code that couples the two widely used tools OpenFoam and PhreeqcRM through the creation of the gwaterFreakFoam library. Benchmarking the newly developed code against existing, well-tested codes demonstrates the accuracy and efficiency of the new code. The major motivation for the development of the new code was to generate a reactive transport code for unstructured grids with both wide-ranging geochemical capabilities and a high accuracy of the transport solution under advection-

dominated conditions, which is currently not available elsewhere. Moreover, the library also allows for the simulation of the diffusion, advection and reactions of gaseous compounds, which adds further to the usefulness of the code and its applications to advanced biogeochemical simulations problems. While not presented here, thermal and/or density effects can also be considered, when required. Based on the generated code structure the utility of the code can easily be further enhanced.

Acknowledgments

The authors acknowledge the detailed work and help of the reviewers to improve the manuscript. We also wish to thank Sorab Panday (GSI) for thorough exchanges on PHT-USG.

Supporting information

Additional details for all discussed cases (geometry, flow transport and reactions parameters, tolerances used for solvers, computational demand) are provided in the SI. The library with instructions for use and test cases are given in https://github.com/oatteia111/muFlowRTFoam. Pre and post-processing for muFlowRT can be done using the free ORTI3D interface (orti3d.ensegid.fr). Supporting Information is generally *not* peer reviewed.

References

André, L., P. Audigane, M. Azaroual, and A. Menjoz. 2007. Numerical modeling of fluid-rock chemical interactions at the supercritical CO2-liquid interface during CO2 injection into a carbonate reservoir, the dogger aquifer (Paris Basin, France). *Energy Conversion & Management* 48, no. 6: 1782–1797.

Appelo, C. A. J., and A. Willemsen. 1987. Geochemical Calculations and Observations on Saltwater Intrusion. I. A combined geochemical/mixing cell model, *Journal of Hydrology* 94, no. 3–4: 313-330,

Appelo, C. A. J., and M. Rolle. 2010. PHT3D: A reactive multicomponent transport model for saturated porous media. *Ground Water* 48, no. 5: 627–632.

Barry, D. A., H. Prommer, C. T. Miller, P. Engesgaard, A. Brun, and C. Zheng. 2002. Modelling the fate of oxidisable organic contaminants in groundwater. *Advances in Water Resources* 25, no. 8-12: 945–983.

Bear, J. 1988. *Dynamics of Fluids in Porous Media*. Dover Civil and Mechanical Engineering Series, Dover USA.

Chen, Z., Huan, G., Ma, Y. 2006. *Computational methods for multiphase flows in porous media.* Soc. of Ind. And App. Math. Philadelphia USA.

Clement, T. P. 1997. RT3D—A modular computer code for simulating reactive multi-species transport in 3-Dimensional groundwater systems. Battelle Pacific Northwest National Laboratory Research Report. *PNNL-SA-28967*.

Darwish, M. S., and F. Moukalled. 2003. TVD schemes for unstructured grids. *International Journal of Heat & Mass Transfer* 46, no. 4: 599–611.

Diersch. 2014. *FEFLOW: Element Modeling of Flow, Mass and Heat Transport in Porous and Fractured Media*. Berlin, Heidelberg: Springer-Verlag.

De Sousa, E. R. 2012. Groundwater modelling meets geochemistry: Building the bridge between FEFLOW and PHREEQC with IFMPhreeqc. In International Mine Water Association Annual Conference vol. 2012.

Dong, Y., and G. Li 2009. A parallel PCG solver for MODFLOW. *Groundwater* 47, no. 6: 845-850.

Engesgaard, P., and K. L. Kipp. 1992. A geochemical transport model for redox-controlled movement of mineral fronts in groundwater flow systems: a case of nitrate removal by oxidation of pyrite. *Water Resources Research* 28, no. 10: 2829-2843.

Geuzaine, C., and J.-F. Remacle. 2009. Gmsh: A three-dimensional finite element mesh generator with built-in pre- and post-processing facilities. *International Journal for Numerical Methods in Engineering* 79, no. 11: 1309-1131.

Harbaugh, A. W. 2005. *MODFLOW-2005: The U.S. Geological Survey Modular Ground-Water Model—The Ground-Water Flow Process*. U.S. Geological Survey Techniques and Methods 6-A16.

Healy, R. W., S. S. Haile, D. L. Parkhurst, and S. R. Charlton. 2018. VS2DRTI: Simulating heat and reactive solute transport in variably saturated porous media. *Ground Water* 56, no. 5: 810-815.

Horgue, P., C. Soulaine, J. Franc, R. Guibert, and G. Debenest. 2015. An open-source toolbox for multiphase flow in porous media. *Computer Physics Communications* 187: 217-226.

Jacques, D., L. Wang, E. Martens, and D. Mallants. 2012. *Benchmarking the CEMDATA07 Database to Model Chemical Degradation of Concrete Using GEMS and PHREEQC*. report of the Nuclear Energy Agency of the OECD (NEA) (No. NEA-RWM-R--2012-3-REV).

Lasaga, A. C., and J. Kirkpatrick. 1981. *Kinetics of Geochemical Processes*. Berlin, Boston: De Gruyter, 1981. https://doi.org/10.1515/9781501508233

Lu, R., T. Nagel, J. Poonoosamy, D. Naumov, T. Fischer, V. Montoya, and H. Shao. 2022. A new operator-splitting finite element scheme for reactive transport modeling in saturated porous media. *Computers & Geosciences* 163: 105-106.

Maes, J., and H.P. Menke 2021. GeoChemFoam: Direct modelling of multiphase reactive transport in real pore geometries with equilibrium reactions. *Transport in Porous Media* 139, no. 2:271-299.

Mangani, L., M. Buchmayr, and M. Darwish. 2014. Development of a novel fully coupled solver in OpenFOAM: Steady-state incompressible turbulent flows. *Numerical Heat Transfer, Part B: Fundamentals* 66, no. 1: 1-20.

Mayer, K.U., E.O. Frind and D. W. Blowes. 2002. Multicomponent reactive transport modeling in variably-saturated porous media using a generalized formulation for kinetically controlled reactions. Water Resources Research 38, no. 9: 1174. doi.org/10.1029/2001WR000862.

McDonald, J. M., and A. W. Harbaugh. 1988. *MODFLOW, a Modular 3D Finite Difference Ground-Water Flow Model*. U.S. Geological Survey Open-File Report 83-875.

Millington, R. J. 1959. Gas diffusion in porous media. *Science* 130, no. 3367: 100-102.

Mualem, Y. 1986. Hydraulic Conductivity of Unsaturated Soils: Prediction and Formulas. In *Methods of Soil Analysis, Part 1: Physical and Mineralogical Methods*: 799-823. Soil Sci. Soc America book series, editor A. Klute

Muniruzzaman, M., and M. Rolle. 2019. Multicomponent ionic transport modeling in physically and electrostatically heterogeneous porous media with PhreeqcRM coupling for geochemical reactions. *Water Resources Research* 55, no. 12: 11121-11143.

Nielsen, D. R., M. T. Van Genuchten, and J. W. Biggar. 1986. Water flow and solute transport processes in the unsaturated zone. *Water Resources Research* 22, no. 9: 89S-108S.

Panday, S. 2017. *Block-Centered Transport (BCT) Process for MODFLOW-USG. GSI Environmental*. https://www.gsienv.com/product/modflow-usg/

Panday, S., C. D. Langevin, R. G. Niswonger, I. Motomu and J. D. Hughes. 2013. MODFLOW–USG version 1: An unstructured grid version of MODFLOW for simulating groundwater flow and tightly coupled processes using a control volume finite-difference formulation. U.S. Geological Survey Techniques and Methods 6A45.

Panday, S., H. Mori, C. M. Mok, J. Park, H. Prommer, and V. Post. 2019. *PHT-USG Module of the BTN Package of MODFLOW-USG Transport. GSI Environmental*. https://www.gsienv.com/product/pht-usg-module/

Parkhurst, D. L., K. L. Kipp, and S. R. Charlton. 2010. *PHAST version 2—A program for simulating groundwater flow, solute transport, and multicomponent geochemical reactions.* U.S. Geological Survey Techniques and Methods 6A35.

Parkhurst, D. L., and C. A. J. Appelo. 2013, Chap. A43. Description of Input and Examples for PHREEQC Version 3—A Computer Program for Speciation, Batch-Reaction, One-Dimensional Transport, and Inverse Geochemical Calculations: U.S. Geological Survey Techniques and Methods 6A43, 497 p.

Parkhurst, D. L., and C. A. J. Appelo. 1999. User's guide to PHREEQC (Version 2): A computer program for speciation, batch-reaction, one-dimensional transport, and inverse geochemical calculations. U.S. Geological Survey Water-Resources Investigations Report 99-4259. https://doi.org/10.3133/wri994259

Parkhurst, D. L., and L. Wissmeier. 2015. PhreeqcRM: A reaction module for transport simulators based on the geochemical model PHREEQC R. *Advances in Water Resources* 83: 176-189.

Pavuluri, S., Tournassat, C., Claret, F., and Soulaine, C. 2022. Reactive Transport Modeling with a Coupled OpenFOAM®-PHREEQC Platform. *Transport in Porous Media*, 145, no. 2: 475-504.

Prommer, H., D. A. Barry, and C. Zheng. 2003. MODFLOW/MT3DMS-based reactive multicomponent transport modeling. *Ground Water* 41, no. 2: 247-257.

Prommer, H., J. Sun, and B. D. Kocar. 2019. Using reactive transport models to quantify and predict groundwater quality. *Elements* 15, no. 2: 87-92.

Robinson, D. B., D. Y. Peng, and S. Y. K. Chung. 1985. The development of the Peng – Robinson equation and its application to phase equilibrium in a system containing methanol. *Fluid Phase Equilibria* 24, no. 1–2: 25-41.

Schafer, D., J. Sun, J. Jamieson, A. Siade, O. Atteia, S. Seibert, S. Higginson, and H. Prommer. 2021. Fluoride release from carbonate-rich fluorapatite during managed aquifer recharge: Model-based development of mitigation strategies. *Water Research* 193: 116880.

Seibert, S., O. Atteia, U. Salmon, A. Siade, G. Douglas, and H. Prommer. 2016. Identification and quantification of redox and ph buffering processes in a heterogeneous, low carbonate aquifer during managed aquifer recharge. *Water Resources Research* 52, no. 5: 4003-4025.

Siade, A.J., B. C. Bostick, O. A. Cirpka, and H. Prommer. 2021. Unraveling biogeochemical complexity through better integration of experiments and modeling. *Environmental Science. Processes & Impacts* 23, no. 12: 1825-1833.

Sliwka, I., M. Opoka, P. Mochalski, T. Kuc, and M. Duli. 2005. Groundwater Dating with 3H and SF 6 in Relation to Mixing Patterns, Transport Modelling and Hydrochemistry. *Hydrological Processes* 2275, no. 2004: 2247-2275.

Sun, H., X. Ji and X. S. Wang. 2019. Parallelization of groundwater flow simulation on multiple GPUs. In Proceedings of the 3rd International Conference on High Performance Compilation, Computing and Communications (pp. 50-54).

Sun, J., M. J. Donn, P. Gerber, S. Higginson, A. J. Siade, D. Schafer, S. Seibert, and H. Prommer. 2020. Assessing and managing large-scale geochemical impacts from groundwater replenishment with highly treated reclaimed wastewater. *Water Resources Research* 56, no. 11.

Van Genuchten, J. 1980. A closed-form equation for predicting the hydraulic conductivity of unsaturated soils 1. *Soil Science Society of America Journal* 8: 892-898.

Van Leer, B. 1974. Towards the Ultimate Conservative Difference Scheme. II. Monotonicity and Conservation Combined in a Second-Order Scheme. *Journal of Computational Physics* 14: 361-370.

Vrettos, N. A., H. Imakoma, and M. Okazaki. 1989. An effective medium treatment of the transport properties of a Voronoi Tesselated network. *Journal of Applied Physics* 66, no. 7: 2873-2878.

Walter, A. L., E. O. Frind, D. W. Blowes, C. J. Ptacek, and J. W. Molson. 1994. Modeling of multicomponent reactive transport in groundwater. 1: Model development and evaluation. *Water Resources Research* 30, no. 11: 3137–3148.

Weller, H. G., G. Tabor, H. Jasak, and C. Fureby. 1998. A tensorial approach to computational continuum mechanics using object-oriented techniques. *Computers in Physics* 12, no. 6: 620.

Xu, T., E. Sonnenthal, N. Spycher, G. Zhang, L. Zheng, and K. Pruess. 2012. Toughreact: A Simulation Program for Subsurface Reactive Chemical Transport Under Non-isothermal Multiphase Flow Conditions. In *Groundwater Reactive Transport Models*: 74-95. Bentham Science Publishers Ltd.

Yeh, G., and V. Tripathi. 1991. A model for simulating transport of reactive multi-species components: Model development and demonstration. *Water Resources Research* 27: 3075-3094.

Zheng, C., and G. D. Bennett. 2002. *Applied Contaminant Transport Modeling*. 2nd edition, Wiley-Interscience, New York.

Zheng, C., and P. P. Wang. 1999. *MT3DMS: A Modular Three-Dimensional Multispecies Model for Simulation of Advection, Dispersion and Chemical Reactions of Contaminants in Groundwater Systems; Documentation and User's Guide*. Contract Report SERDP-99 vol. 1. Vicksburg, MS: U.S. Army Engineer Research and Development Center.

Zheng, C. 1990. *MT3D, A Modular Three-Dimensional Transport Model for Simulation of Advection, Dispersion, and Chemical Reactions of Contaminants in Groundwater*

Systems, Report to the Kerr Environmental Research Laboratory. Ada, OK: United States Environmental Protection Agency.

Zheng, C., M. C. Hill, G. Cao, and R. Ma. 2012. MT3DMS: Model use, calibration, and validation. *Transactions of the ASABE* 55, no. 4: 1549-1559.

Figure 1. Overall structure of the muFlowRT library and solvers to treat reactive transport.. $\boldsymbol{\phi}$ stands for porosity, ρ the density μ the viscosity, φ the fluid flux, p is the pressure, S the saturation, C the concentration, and T the temperature, where w is for water and g for gas phase, i stands of the component index. In ovals, *Eq* represents the equations. For the exchange with Phreeqc, *gmol* is the number of moles of each gas component in the gas phase and $\delta_{mineral}$ is the amount of minerals precipitated or dissolved.

Figure 2. Comparison of the various tested numerical solutions with the corresponding analytical solution for an instantaneous tracer pulse in a diagonal flow field. a: concentration profile in longitudinal direction, b: in transverse direction. Here muRT results are shown for two different Openfoam advection schemes: van Leer (vl) and SuperBee (sb)scheme.

Figure 3. Vertical profiles of water saturation (left) at time 3 and 5 days, and partial pressure of the gases (middle t=3 days and right t=5 days) involved in benzene diffusion and biodegradation. Solid lines: MIN3P, dash-dotted lines muRT. Initial equilibration is for a steady water content profile with freewater level at z=0.01 m.

Figure 4. Head contours in layers 1 to 4 (top to bottom and left to right) of the 3D model (contours for 9, 18, 27, 40 and 50m), muRT in solid lines, MODFLOW-USG dash-dotted lines. Coordinates are in m. in layer 2 the positions of specified heads are provided in greyed polygons, and the drain as grey dashed polygon. Model details are provided in SI.

Figure 5. Contour maps of tracer concentrations after a 50y simulation time. Solid lines represent muRT results while dashed lines show the results for MODFLOW-USG. The grey area shows the location of the constant source zone (in layer 1).

Figure 6. Spatial distribution of F (left) and P (right) from layer 2 to layer 4 (top to bottom). Solid lines for muRT and dotted ones for MODFLOW-USG. Contours lines are shown for 6×10^{-6}, 2×10^{-5}, 8×10^{-5} mol/L for F and for 4×10^{-6},1×10^{-5}, and 3×10^{-5} for P.

Figure 7. a: Water saturation (blue) and pH (red lines) as a function of radial distance (m) from the injection well. b and c: Simulated concentration profiles of selected species (in mol/L) after 10 years of continuous gas injection. Continuous lines for TOUGHREACT and dash-dotted lines for muRT.

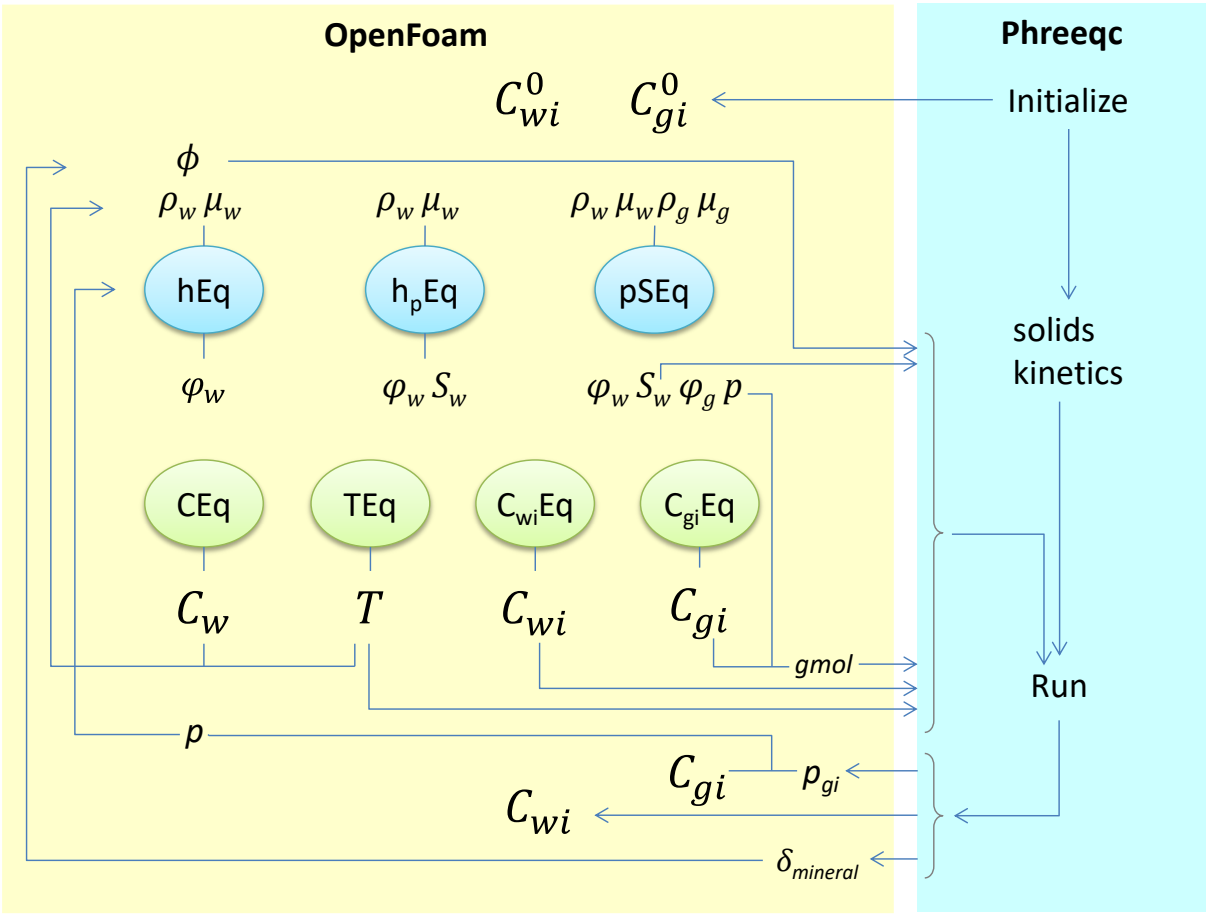

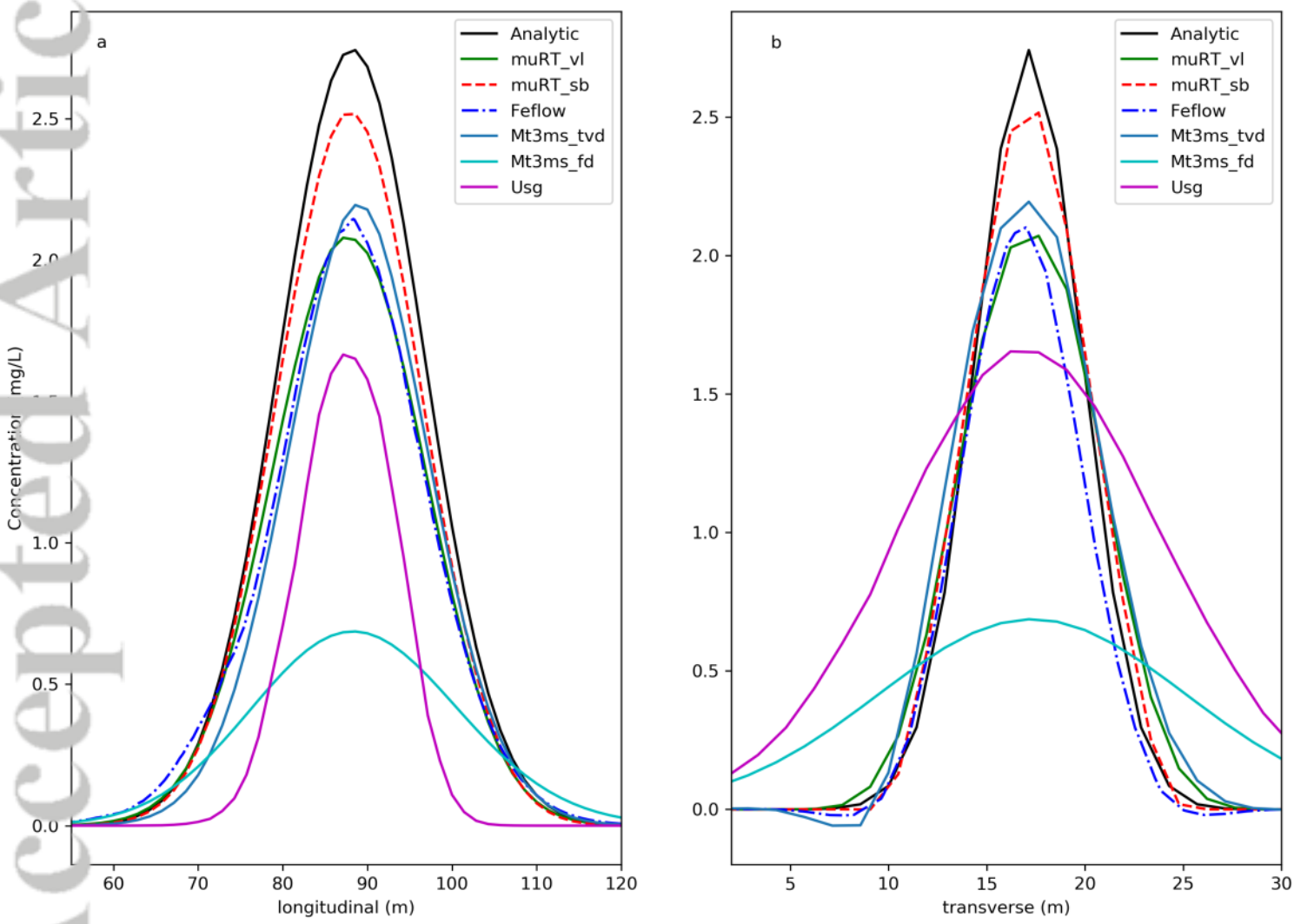

Figure2.png

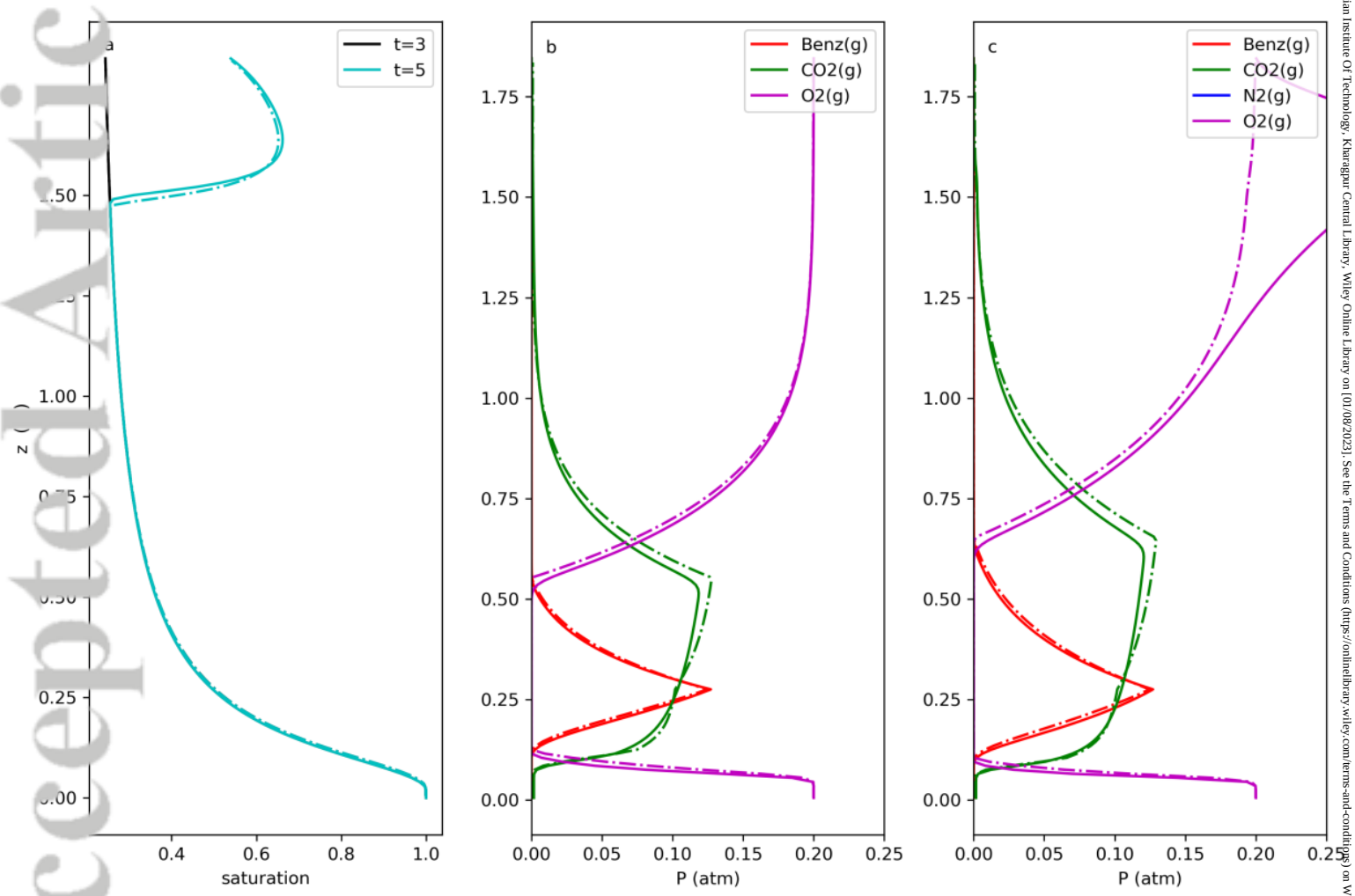

Figure3.png

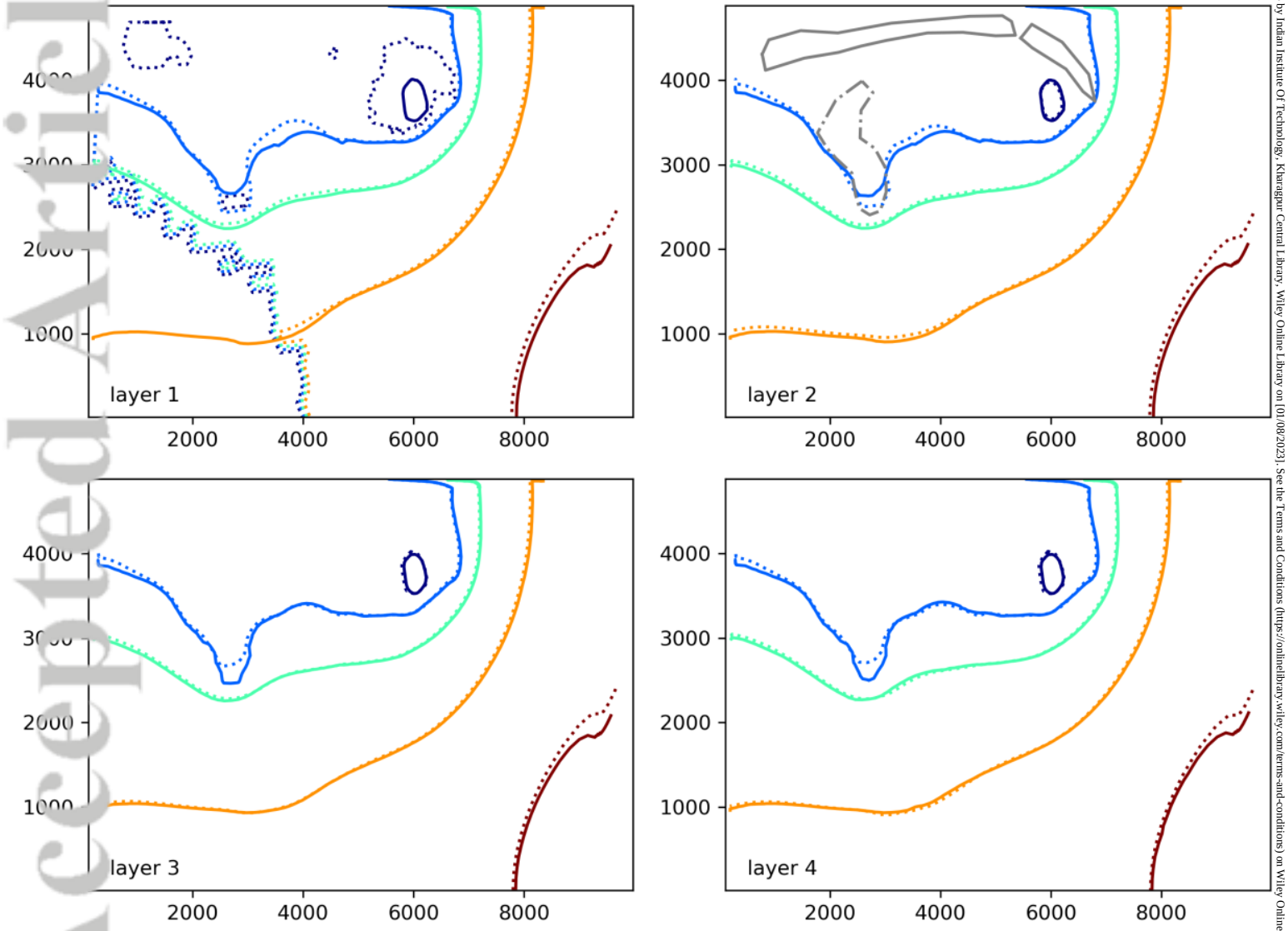

Figure4.png

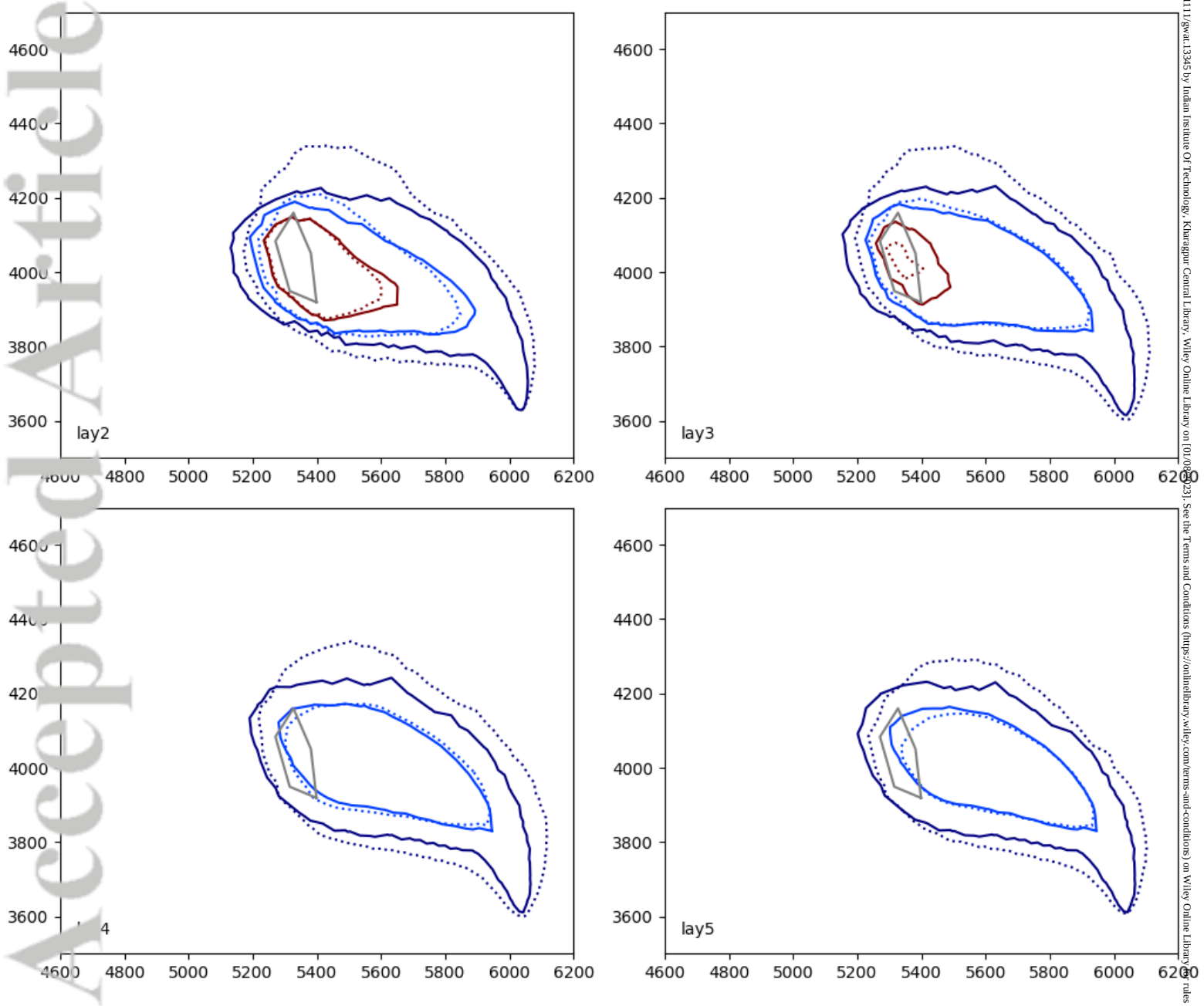

Figure5.png

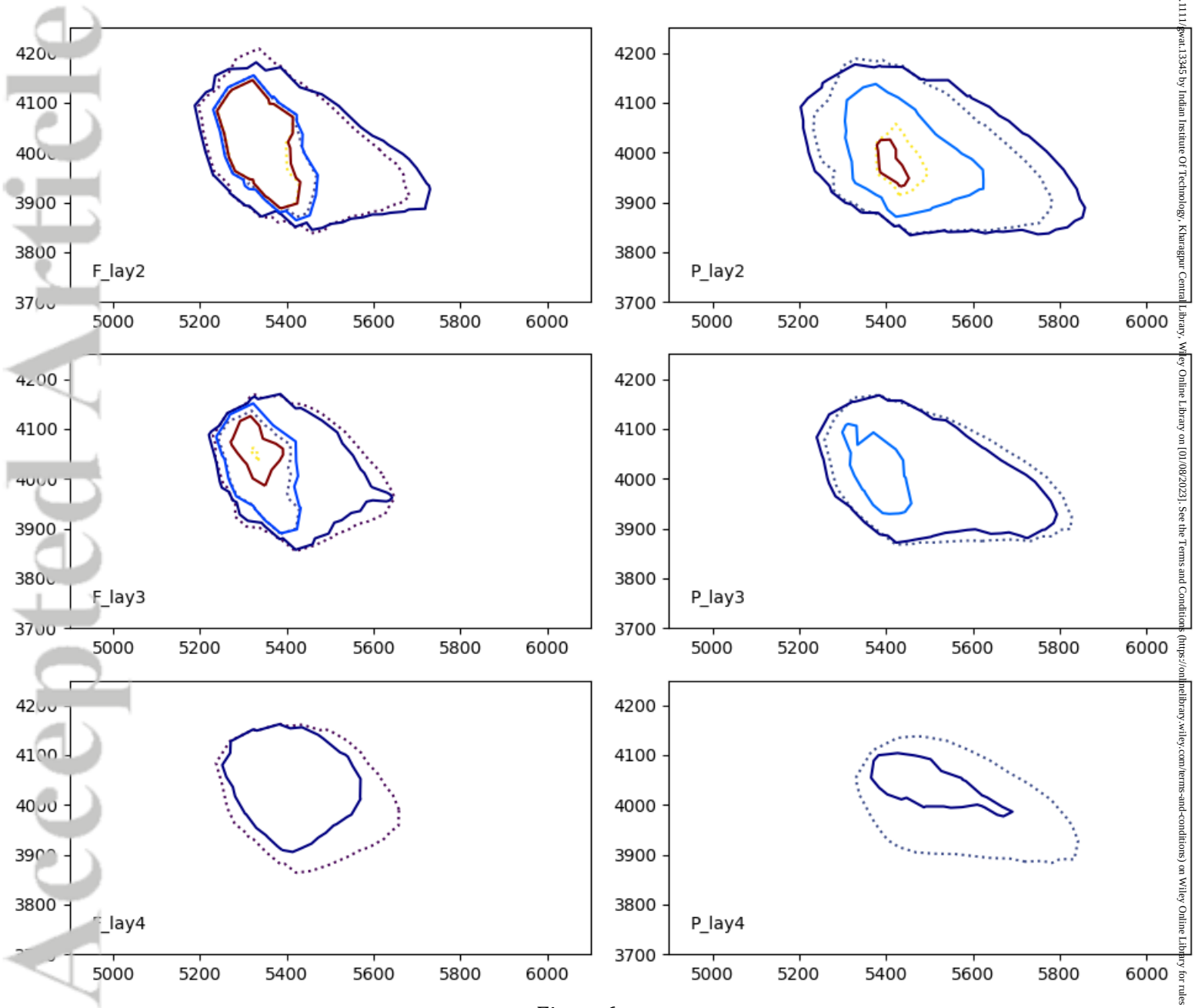

Figure6.png

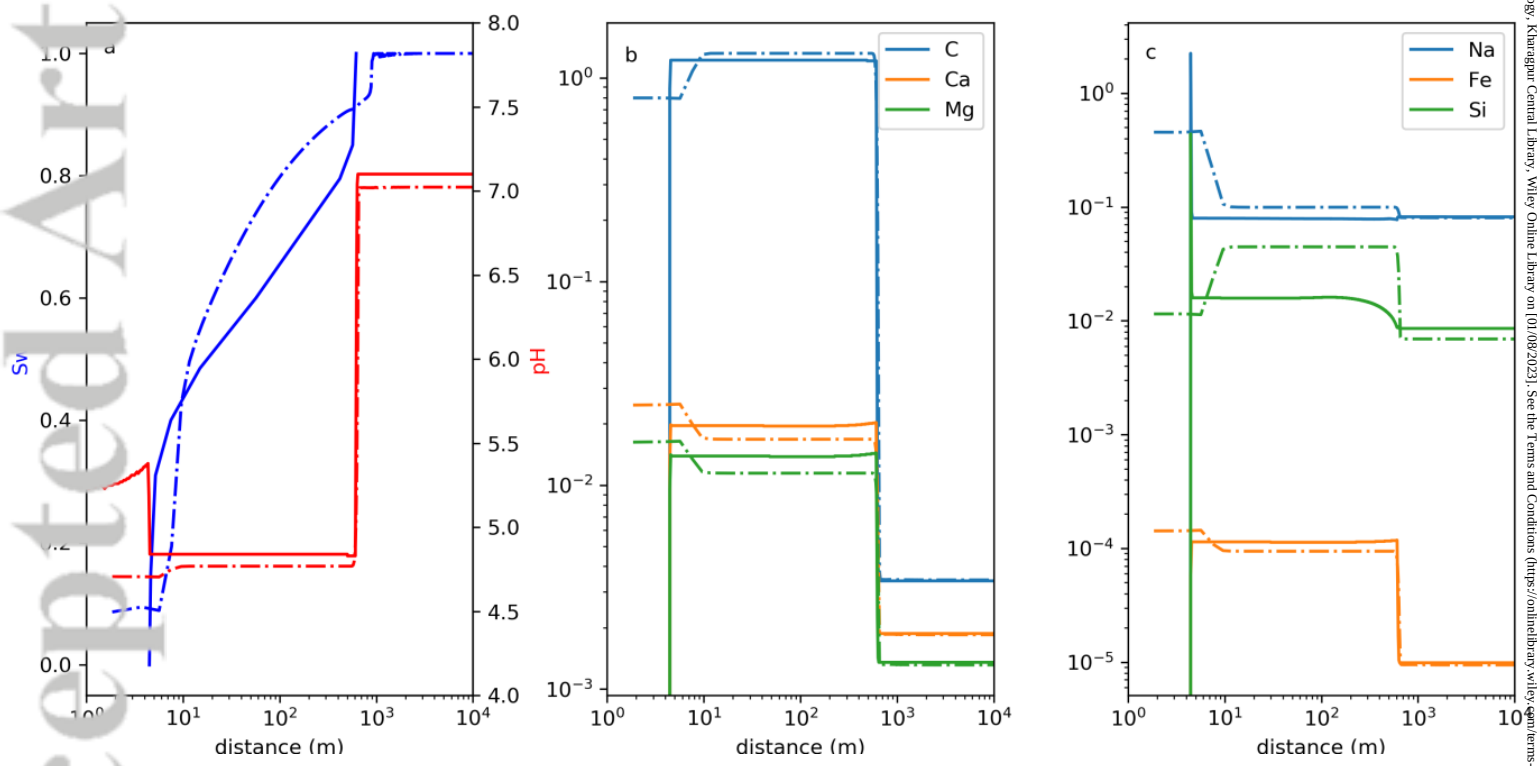

Figure7.png